Magazine of Civil Engineering

ISSN 2712-8172

journal homepage: http://engstroy.spbstu.ru/

Research article

UDC 666.91

DOI: 10.34910/MCE.133.2

Influence of electric current on the mineral matrix of technogenic anhydrite

A.N. Gumeniuk[1] , ***A.F. Gordina***[1] , ***S.M. Petrynin***[1] , ***A.F. Buryanov***[2] ✉ , ***V.Y. Skeeba***[3]

[1] *Kalashnikov Izhevsk State Technical University, Izhevsk, Russian Federation*

[2] *Moscow State University of Civil Engineering (MGSU) National Research University, Moscow, Russian Federation*

[3] *Novosibirsk State Technical University, Novosibirsk, Russian Federation*

✉ *rga-service@mail.ru*

Keywords: fluoroanhydrite, modification, carbon fiber, mineral matrix, microstructure, composite materials, electrical properties, electrochemical corrosion, micro heating elements

Abstract. The current conditions for the development of industrial and civil engineering in the regions with a negative average daily temperature require an increase in the economic efficiency of heating systems and reduction of the material consumption for its production and operation. One of the solutions to this problem is electrically conductive concrete. Cost reduction is achieved through the use of binders of anthropogenic origin. The electrically conductive concrete samples with dimensions of 70 × 70 × 70 mm and prototype product with dimensions of 500 × 500 × 50 mm were used for the assessment of the effect of the micro heating elements on the performance and physicochemical properties of mineral matrix. The electrically conductive concrete was based on waste of anthropogenic origin (fluorine-anhydrite) and fine aggregates. The additives in the form of 7 % technical soot suspension and 1 % of carbon fiber were used as micro heating elements. The physical and technical studies were carried out on the 28th day after 3 cycles of heating and cooling of the samples. The obtained results confirm that carbon fiber reduces the specific volume resistance up to 8.5 kOhm·cm. It allows the usage of proposed compositions for the manufacture of large-format heating elements. The experimental operation of large-format heating elements based on the developed compositions made it possible to determine its thermophysical characteristics. The heating of the elements surface from 21.9 to 28.5 °C for 40 minutes were obtained. Thus, the use of the developed prototype as heating elements is possibly provided that the pre-installed electrodes are protected from electrochemical corrosion. The electrochemical corrosion must be established through the use of methods of physicochemical analysis.

Funding: Investigations were performed on the equipment of Core Shared Research Facilities “Center of physical and physical-chemical methods of analysis, investigations of properties and characteristics of surface, nanostructures, materials and products” of Udmurt Federal Research Center of UB RAS

Citation: Gumeniuk, A.N., Gordina, A.F., Petrynin, S.M., Buryanov, A.F., Skeeba, V.Y. Influence of electric current on the mineral matrix of technogenic anhydrite. Magazine of Civil Engineering. 2025. 18(1). Article no. 13302. DOI: 10.34910/MCE.133.2

1. Introduction

Modern trends in the development of electrotechnical concretes, which traditionally consist of aggregates with rationally selected granulometric composition, binder (Portland cement) and modified with

carbon-containing components of various morphological structures, are aimed at increasing of economic efficiency and environmental friendliness [1, 2]. The electrically conductive concrete based on Portland cement is the most common type of electrotechnical concrete due to its technological advantages, such as workability, strength, and durability. At the same time, the current intensification in civil engineering, infrastructure development, and urbanization have led to the widespread use of concrete and reinforced concrete on Portland cement and its negative impact on the environment [3, 4]. Production of cement and steel causes a significant CO_2 emission [4]. Environmental monitoring of industrial enterprises of the cement industry shows that every kilogram of produced Portland cement emits about 0.70–0.85 kg of carbon dioxide [4, 5]. The tendency of global industrial production makes it possible to forecast a volume of 5.8 billion tons of cement by 2030 [5, 6].

It has led to the development of research in the field of electrotechnical concretes aimed at solving problems of reducing the environmental burden by recycling of industrial waste in the production of environmentally friendly materials-substitutes for Portland cement [7, 8].

The associated industrial products (gypsum-containing waste), such as products of chemical, forestry, and mining industries, are the potential source of raw materials for the production of electrotechnical concretes. The annual volume of gypsum-containing waste for 2023 is about 100–280 million tons per year [7]. Global volumes of solid gypsum-containing waste are estimated from 7 to 8 billion tons [8]. This type of waste includes phosphogypsum, borogypsum, fluorohydrite, citrogypsum, titanogypsum, and others. One of the common gypsum-containing wastes is fluoranhydrite [4, 5]. This solid sulfate-containing production waste is formed as a by-product in the production of hydrogen fluoride. The technology for producing hydrogen fluoride is based on the interaction of fluorspar with 98 % sulfuric acid according to the reaction:

$$CaF_2 + H_2SO_4 = 2HF + CaSO_4.$$

The crushed fluorspar is mixed with sulfuric acid, and the resulting mass is fed into rotary kilns. At 160–280 °C, the gas leaving the kiln contains up to 80 % of HF [5, 6]. The product discharged from the kiln contains more than 80 % of $CaSO_4$, 0.5–5.0 % of CaF_2, 10–12 % of H_2SO_4, 1.5–4.0 % of SiO_2, and 0.5–1.5 % of R_2O_3 [6].

In the works of A.A. Ponomarenko and Yu.G. Meshcheryakov [7], the composition of the by-product of the production of HaloPolymer JSC (Perm) after 3–5 years of storage was established to include no less than 20 % of γ-$CaSO_4$; up to 78 % of β-$CaSO_4$; from 1.0 to 1.8 % of CaF_2; from 0.5 to 10.0 % of H_2SO_4; up to 0.2 % of HF.

The water-soluble fluoride and sulfate ions in the composition, as well as suspended matters, have a negative impact on the environment when fluoroanhydrite accumulates in sludge storage facilities and when discharged into water bodies [7, 8].

To reduce the negative impact, several directions for the utilization of sulfate-containing waste have been developed: production of sulfuric acid and lime; of anhydrite binder; of gypsum binder; use as a regulator of the setting time of binders [8, 9].

Today, one of the most common and studied directions is the production of a binder by crushing, subsequent grinding, and milling of coarse-grained fluoroanhydrite stone. The resulting dispersed powder is mixed with a rationally selected solution of water with a hydration catalyst, which can be sodium sulfate, iron sulfate, potassium bisulfate, blast furnace slag, alumina sulfate, and others [10].

In the countries, such as the People's Republic of China, the United States of America, and the Russian Federation, leading in the volume of accumulation of gypsum-containing waste, this binder has found quite wide application in the building materials industry [9].

Fluoroanhydrite and anhydrite binders are actively used in the production of various materials and products, including cement-free concrete and mortars [9, 10], facing and thermal insulation materials [1, 8].

The research by Russian and Chinese scientists [11] has shown the possibility of using such binders in the production of hollow and cellular blocks. Iron, sodium, and potassium sulfates have been successfully tested as hardening activators.

A sulfate-containing binder, with an optimal selection of a hardening activator, is technologically highly adaptable to modification by introducing extra additives to expand the functional properties of products. Thus, the use of carbon-containing additives made it possible to experimentally test products based on fluoroanhydrite with a relatively low specific resistance [12, 13].

In the last decade, a significant number of research works have been devoted to the formation of electrically conductive properties in mineral matrices by reducing the percolation threshold, which makes it

possible to expand the scope of application and create products with a resistive self-heating function [14]. To justify the possibility of producing these products and ensuring the required specific resistance, various models have been proposed that justify the formation of electrically conductive paths in the matrix volume, such as cluster [6], linear [15], and complex [16]. To ensure various forms of electrically conductive paths, the use of additives of various morphology [17] and composition [18] has been proposed. The research results have confirmed the effectiveness of additives based on carbon-containing materials with various morphological features, including finely dispersed industrial soot and carbon fiber [19]. In this case, various types of metal products made of structural or stainless steel, such as reinforcement, plates, pipes, are used to supply electric current to the samples [20].

It is known [21] that the mechanism of electrical conductivity in mineral matrices, such as concrete based on Portland cement or gypsum, is based on ionic conductivity. In ionic conductors, such as electrolytes, ions move under the influence of an electric field. To transfer charge in a mineral matrix, there must be an electrolyte containing charged particles [21] located in pores, voids, in contact zones, and in the matrix [22].

In a mineral matrix based on industrial anhydrite, the presence of electrolyte in the structure depends on the humidity, particle size, their mutual arrangement, and also on the wedging pressure acting in thin layers. Pellicular moisture is several tens of angstroms thick and mainly limits the electrical conductivity of the system [23], moisture in pores and voids is represented by relatively large inclusions isolated from each other and does not make a noticeable contribution to the electrical conductivity of the matrix [23].

In countries with a dry climate, slabs and blocks made of dense mixtures based on gypsum binders are actively used in the construction of walls and partitions [17, 20, 23]. With an average density of 1500–1800 kg/m^3, gypsum concrete products have the required strength properties. Due to a number of reasons, prefabricated gypsum concrete products have not found wide application in housing construction.

The load-bearing capacity of gypsum concrete masonry can be increased by reinforcement: steel mesh, rods [15, 20]. However, steel reinforcement is known to actively corrode when in contact with hydrated gypsum binder [22, 23].

From the data presented in the study [15, 20, 22], it follows that the pH decreases during the hardening of the mineral matrix. The change in pH is observed immediately after the binder is mixed. Also in the works [24, 29], it was established that the presence of sulfates allows the pH to decrease during the first 30 minutes, before the formation of the crystalline structure.

In this regard, during the formation of the mineral matrix in a pre-reinforced product or a product with pre-installed electrodes, an oxide film is formed on the surface of the reinforcement, which is similar to the mechanism of formation of an inhibiting film during the manufacture of reinforced concrete [24, 25]. The subsequent decrease in pH to an acidic environment does not allow the formation of the required thickness of the oxide film on the surface of the reinforcing element [26]. As a result, the presence of bound and free water molecules in the composition of the hydrated sulfate-containing binder determines the emergence of conditions for electrochemical corrosion of iron, a destructive process of metal fracture in liquid conductive media [27, 28].

During the corrosion process in the mineral matrix, under the influence of the corrosion current, the metal dissolves due to electrochemical interaction with the electrolyte. The surface of the metal in the electrolyte is electrochemically heterogeneous, which leads to the formation of microgalvanic corrosion elements [25, 26]. On some areas of the surface, called anodes, the following reaction takes place:

$$\mathrm{Me} \leftrightarrow \mathrm{Men}++\mathrm{n}\bar{\mathrm{e}}.$$

On other areas called cathodes, the following reactions take place:

– in neutral medium

$$\mathrm{O_2} + 2\mathrm{H_2O} + 4\bar{\mathrm{e}} \leftrightarrow 4\mathrm{OH}^{-};$$

– in acid medium

$$2\mathrm{H}++2\bar{\mathrm{e}} \leftrightarrow \mathrm{H_2}\uparrow.$$

The corroding elements of the circuit, being in an open state, corrode on the anodic and cathodic sections in the forward and reverse directions at the same rate. This is due to the fact that a potential difference arises between the metal and the electrolyte solution, associated with the formation of a double electric layer, i.e. an asymmetric distribution of charged particles at the phase boundary [25, 27].

In turn, the electrode potential of metals, calculated using the Nernst thermodynamic equation, depends on the nature of the electrolyte and the ambient temperature [26, 28]. Studies have shown that the corrosion process of a steel rod occurs actively in both acidic and alkaline electrolytes.

The considered features predetermined the need to assess the effect of electric current on a modified mineral matrix during heating and simulating the operation of a product based on a modified fluoroanhydrite binder.

The purpose of this work is to study the processes occurring in a modified mineral matrix based on fluoroanhydrite when passing electric current through structural reinforcement and to assess the performance of the contact zone “steel reinforcement/mineral matrix” after several heating/cooling cycles.

The results obtained will allow us to assess the possibility of solving the current problem of recycling large-tonnage chemical production waste by offering effective compositions and technical solutions for the production of heating elements.

2. Materials and Methods

Binder. The used fluoroanhydrite was provided by HaloPolymer LLC, Perm, Russia. The chemical composition of the binder is as follows: SiO_2 – 3.5 %; Al_2O_3 – 0.7 %; Fe_2O_3 – 0.95 %; CaO – 37 %; SO_3 – 54.42 %; impurities – 3.43 %. According to X-ray phase analysis, fluoroanhydrite is represented by anhydrite (d = 3.50; 2.85 Aº), gypsum (d = 4.29; 3.81 Aº), and calcium carbonate (d = 3.04 Aº) [7, 8]. In production, ground limestone is used to neutralize the binder, due to which the material has the following potential material composition: $CaSO_4$ – 74.78 %; $CaSO_4 \cdot 2H_2O$ – 13.38 %; $CaCO_3$ – 11.00 %; CaF_2 – 0.82 %; H_2SO_4 – 0.02 % [7].

Hydration catalyst. Based on the analysis of scientific research literature and the results of previous studies, sodium sulfate was selected to be introduced in an amount of 2 % of the mass of the binder in order to activate and intensify the processes of hydration and hardening, as well as to obtain the optimal structure of anhydrite stone [10, 6].

Fine aggregate. To ensure the density of the mineral matrix and homogenization of the fiber in the volume of the material, a fine aggregate in the form of quartz sand with a fineness modulus of 0.7 was introduced.

Monsterfiber carbon fiber. To ensure electrically conductive characteristics, uniform heating of the product, and temperature gradient, carbon fiber was introduced, which is also a reinforcing filler. The modifier is a crushed chopped carbon thread, which is obtained by multi-stage heat treatment of PAN fibers (polyacrylonitrile-based fibers) at temperatures up to 320 °C. Technical characteristics of carbon fiber: tensile strength of fiber not less than 3000 MPa; tensile modulus of elasticity of the fiber not less than 230 GPa; density from 1.68 to 1.80 g/cm^3; fiber stretching test not less than 0.8 %; moisture 0.1 %. The production is certified according to the following standards: ISO 9001, OHSAS 18001, ISO 14001.

Plasticizer (Stahement-2000-M). Uniform distribution of carbon fiber in the structure of the mixture is due to a new generation hyperplasticizer (Group I) based on polycarboxylates. The additive is available in liquid form and complies with EN 934-2:2010. Stahement 2000-M is used to obtain highly mobile, including self-compacting, concrete mixtures, for the production of thin-walled and densely reinforced, vertically molded products, complex-configuration structures with a high degree of factory readiness, monolithic reinforced concrete structures, lightweight concrete, monolithic floors, and roads.

Compositions and methods of testing and research. To study the features of the process of heating products, fluoroanhydrite plates 500 × 500 mm were manufactured. Their compositions are presented in Table 1.

Table 1. Component ratio of compositions.

Compositions	Binder (Fluoroanhydrite), kg	Fine aggregate (Fine sand Russian State Standard GOST 8736, Mk=0.7), kg	Hardening activator (Sodium sulfate, Russian State Standard GOST 4166), %	Carbon fiber (Monsterfiber C), %	Plasticizer (Stahement-2000-M), %	Water-to-Binder Ratio
Control	6.961	1.168	2	–	0.5	0.3
AE-1				0.3		0.3
AE-2				0.4		0.3
AE-3				0.5		0.35
AE-4				0.75		0.4

After gaining strength (28 days), studies were conducted on the physical, mechanical, chemical, and thermal properties of the developed compositions and products.

Mechanical strength. The mechanical compressive strength was determined on samples 70 × 70 × 70 mm at the age of 7, 14, and 28 days on a PGM-100MG4-A hydraulic press with a loading rate of 0.5–0.8 MPa/s.

Specific volume resistance. The specific volume electrical resistance was determined on samples of 70 × 70 × 70 mm. The value was calculated according to the formula:

$$\rho = R \cdot A/L,\ \Omega \cdot \text{cm},$$

where ρ is specific resistance of the sample; R is resistance of the sample, determined by measuring with a two-contact method using an E7-20 immittance meter; L is distance between the probes; A is cross-sectional area of the sample. The scheme used for measuring the specific volume resistance is presented in the paper study [29].

Differential scanning calorimetry. The influence of heating and micro heating modifying elements (carbon fiber) on the phase composition of the studied samples was analyzed by means of DSC analysis. The data were obtained on a TGA/DSC1 device of Mettler-Toledo Vostok CJSC, Switzerland, at the temperature range from 60 to 1100 °C at a temperature increase rate of 30 °C/min in an air atmosphere.

Scanning electron microscopy SEM-EDS. The microstructure of the samples was studied using a Thermo Fisher Scientific Quattro scanning electron microscope, Thermo Fisher Scientific Inc, USA. The samples for SEM-EDS analysis were cubic (an edge of 0.5 cm) and were selected using an angle grinder with a diamond disk. No preliminary preparation of the samples by spraying was performed.

Thermophysical characteristics. The thermophysical properties were assessed based on the research results obtained during the development of electrically conductive concrete [30, 31]. The test method involves generating electrical heat by supplying direct current with U = 120 V and I = 3 A to the electrodes according to the diagram shown in Fig. 1. The electric current was supplied until the maximum surface heating temperature of 30 °C was reached. This temperature threshold is due to the fact that during the exploratory stages of the experiment, heating the products above 35 °C was accompanied by the release of water from the volume of the products.

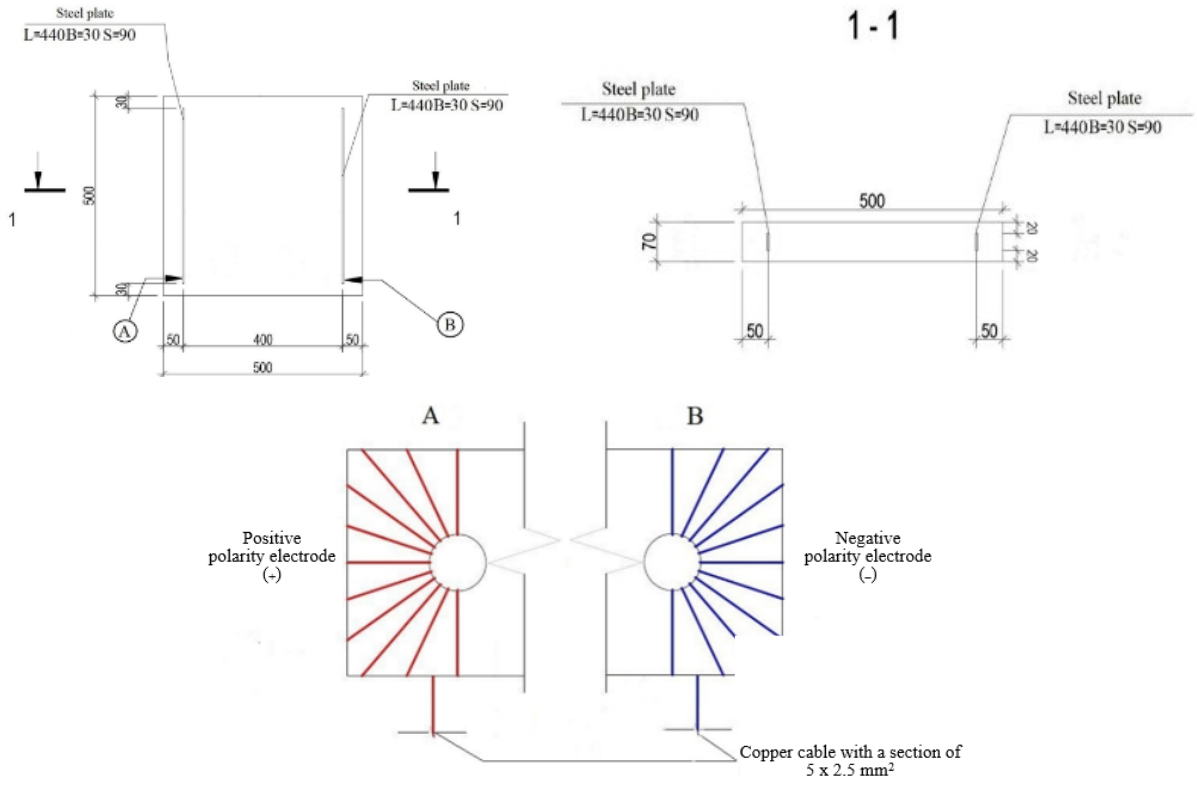

Figure 1. Layout of steel plates in the experimental product (plate).

The change in temperature and its distribution over the surface of the product were recorded using a Guide D192M thermal imaging camera. The intelligent thermal camera of the D series is equipped with a 4-inch high-brightness touch screen, IR resolution of 192 × 144, detector type of 25 μm, temperature range: –20 °C~150 °C, 100 °C~650 °C, 650 °C~1500 °C, accuracy: ±2 °C or ±2 % of readings (at an ambient temperature of 15 to 35 °C and an object's temperature above 0 °C).

3. Results and Discussion

3.1. Analysis of Physical and Technical Properties and Specific Volume Resistance

The analysis of the mechanical strength of the studied compositions shows that the strength of the AE-4 composition in the control test periods is higher than that of the AE-1, 2, 3 compositions by an average of 9.5 %. In turn, on the 28th day of hardening, the strength of the AE-4 composition was 24.2 MPa, which exceeds the strength of the control composition by 7.5 %, the variation coefficient was 7.2 %. After that, the set of properties was determined for the optimal strength of the AE-4 composition.

The results obtained in determining the specific volume electrical resistance of the samples and the change in the parameter during strength gain are shown in Fig. 3. It was found that the specific volume resistance of the control sample corresponds to the parameters given in the literary sources [40, 41] and is 27.1 kOhm·cm on the 28th day. At the same time, the specific volume resistance of the optimal conductive composition with carbon fiber on the 28th day is 8.5 kOhm·cm. This value is 1.5 times lower than that of compositions based on fluoroanhydrite binder modified with a suspension of industrial carbon black, developed and studied in previous works [31–34]. The achieved characteristics are due to the formation of a linear network of conductive elements in the form of uniformly distributed carbon fiber in the volume of the mineral matrix [35–38]. The percolation transition zone is overcome by increasing the breakdown voltage, which allows achieving optimal characteristics in comparison with the results presented in [39–41]. Thus, in [15], for the optimal composition, the specific volume resistance was 13.6 kOhm·cm, and the strength was 35.81 MPa. When gaining strength, an increase in the parameter of specific volume electrical resistance is observed for the control and modified compositions, which is associated with the continued formation of the matrix structure and a decrease in the volume of unbound water [42, 43].

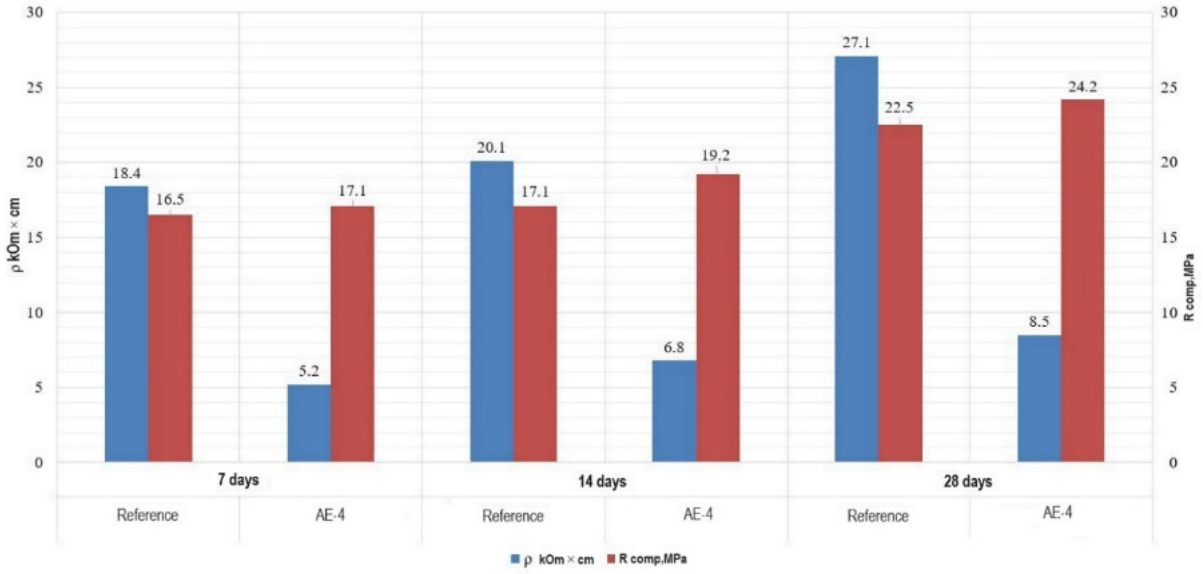

Figure 2. Test results of the control and optimal composition AE-4: mechanical compressive strength, MPa (red); specific volume resistance, kOhm·cm (blue).

Subsequently, the AE-4 composition was used to determine the thermophysical and physicochemical properties and characteristics, as well as to test the heating scheme for the products.

3.2. Study of Thermophysical and Physicochemical Properties

Analysis of data in the field of practical implementation of conductive composite products allows us to determine the parameters of direct current supplied to metal electrodes. Current characteristics varied for current strength I from 0 to 5 A, for voltage U from 0 to 220 V; achieving a uniform temperature gradient over the surface of the product was considered optimal.

The final values ensuring uniform heating were: I = 3A; U = 120V. These characteristics are cost-effective and safe for use in industrial and civil construction. Fig. 3 shows the results of thermophysical tests of a plate with geometric dimensions of 500 × 500 × 50 mm, made of AE-4 composition. The electrodes in the plate were located at a distance of 40 cm from each other, and the dimensions of the electrodes were 44 × 3 cm, installed according to the diagram shown in Fig. 1. Over 40 minutes, the temperature of the product increased uniformly. The maximum temperature of the product after 40 minutes was 31.1 °C, which is 9.2 °C higher than the initial surface temperature. The average power consumption was 660 W/m^2.

a

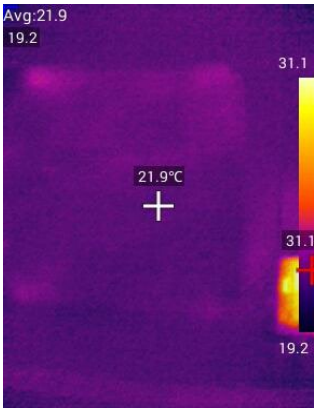

b

Emissivity– 0.75;

Ambient temperature T = 19.2 °C;

Average surface temperature of the plate T = 21.9 °C

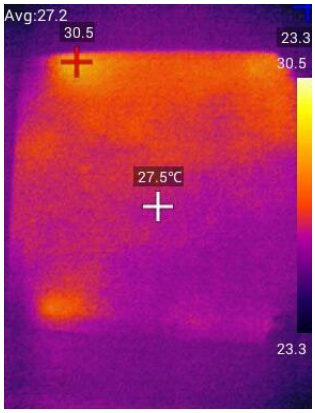

c

Emissivity– 0.75;

Ambient temperature T = 23.3 °C;

Average surface temperature of the plate T = 27.5 °C

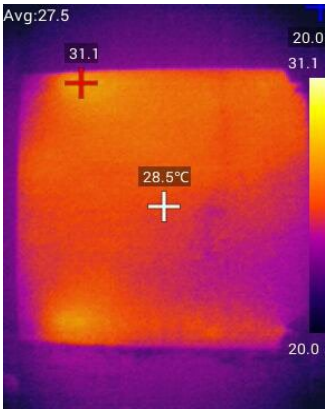

d

Emissivity– 0.75;

Ambient temperature T= 20 °C;

Average surface temperature of the plate T = 28.5 °C

Figure 3. Product and thermal imaging camera images obtained during heating at 20-minute intervals: a – general appearance of the product; b – initial surface temperature of the product; c – temperature 20 minutes after the start of heating; d – temperature 40 minutes after the start of heating.

To assess the effect of heating on the structure of the modified matrix based on the AE-4 composition, a microstructure analysis was performed. The samples were taken on the 28th day of hardening, after several cycles of heating the product to the maximum temperature and subsequent cooling, from different zones, depending on the location of the matrix relative to the heated element, according to Fig. 4.

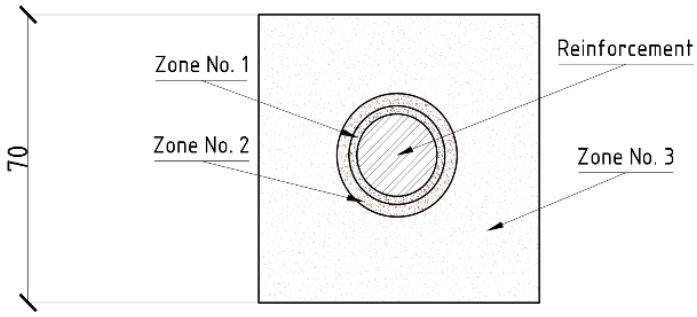

Figure 4. Scheme of sampling for studies of the physical and chemical properties of an electrically conductive composition after several heating/cooling cycles.

The study of the contact zone of the metal and the fluoroanhydrite-based mineral matrix shows a low degree of adhesion (Fig. 5a), which is caused by the formation of lamellar crystals of iron oxide between the mineral matrix and the reinforcement (Figs. 5b and 5d), which are formed in the initial stages of hardening, up to 10 days. In turn, the mineral matrix, including iron oxide, is characterized by a fairly loose structure (Fig. 5c).

Analysis of the microstructure of the mineral matrix, taken from Zone No. 2, remote from direct contact with the metal, shows the presence of poorly soluble iron (III) hydroxide (Figs. 6a and 6b). At the same time, thermal influence on cubic crystalline new formations (Fig. 6c) leads to the deformation of the crystals and the appearance of parallel oriented microcracks, promoting the stratification of hydration products (Fig. 6d).

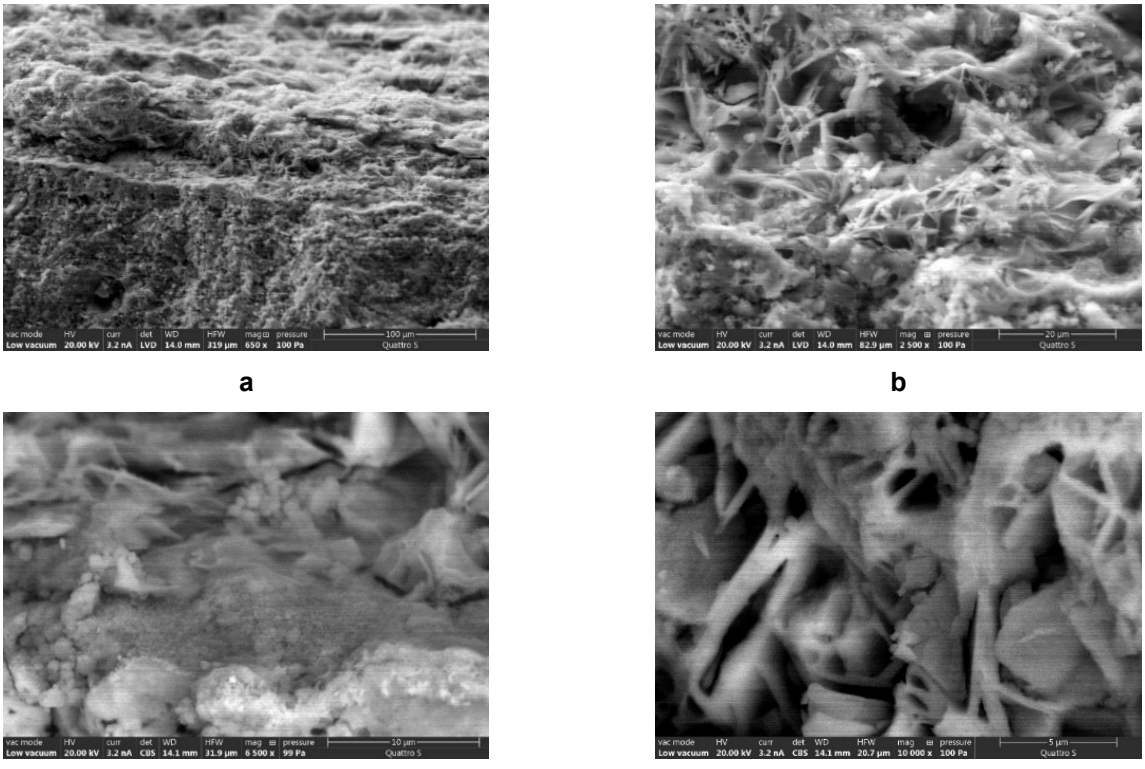

a **b**

c **d**

Figure 5. SEM of the modified AE-4 sample, sampling Zone No. 1, the area of direct contact of the steel rod (reinforcement) and the mineral matrix at different magnifications: a – 650x; b – 2500x; c – 6500x; d – 10000x.

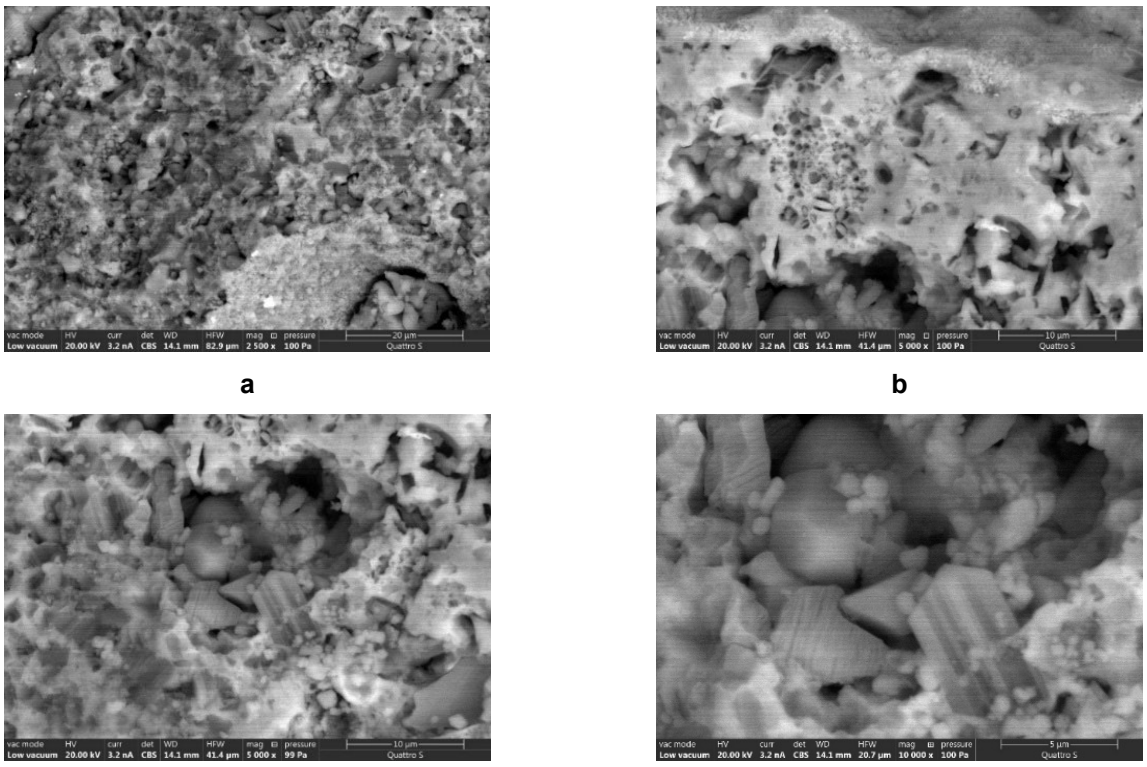

a b

c d

Figure 6.SEM of modified sample AE-4, sampling Zone No. 2, at different magnifications: a – 650x; b, c – 5000x; d – 10000x.

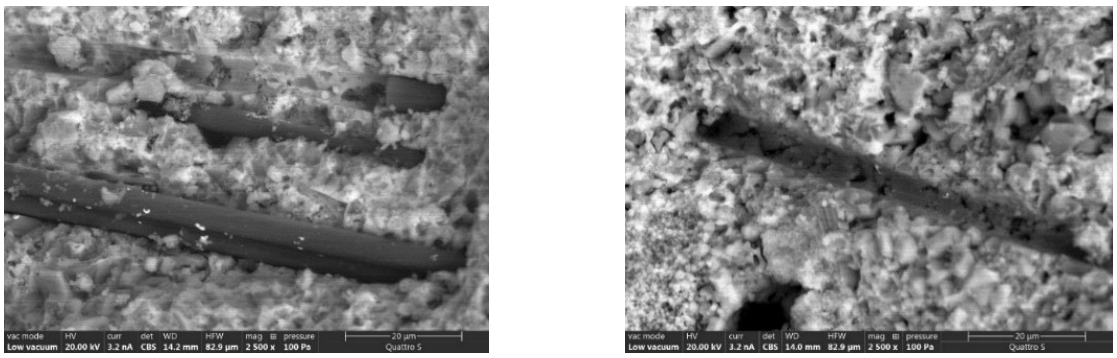

a b

Figure 7.SEM of AE-4modified sample, sampling zone No. 3, at magnifications of 2500x .

Microstructure of the sample taken from Zone No. 3, typical for the modified composition outside the contact zone with the metal element. The presence of carbon fiber uniformly distributed in the volume of the material is noted. The uniformity of distribution is due to the use of a plasticizer and fine filler and the optimality of the composition production (Fig. 7a). At the same time, the absence of chemical interaction in the area of the contact zone of the carbon fiber and the matrix is noted, which is confirmed by the absence of new formations on the surface of the modifier (Figs. 7a and 7b).

To estimate the volume of the matrix structure subject to changes due to heating of the metal reinforcement and to analyze the depth of migration of iron ions into the contact zone of the material around the heating element, the migration of iron ions was analyzed by means of mapping (Fig. 8).

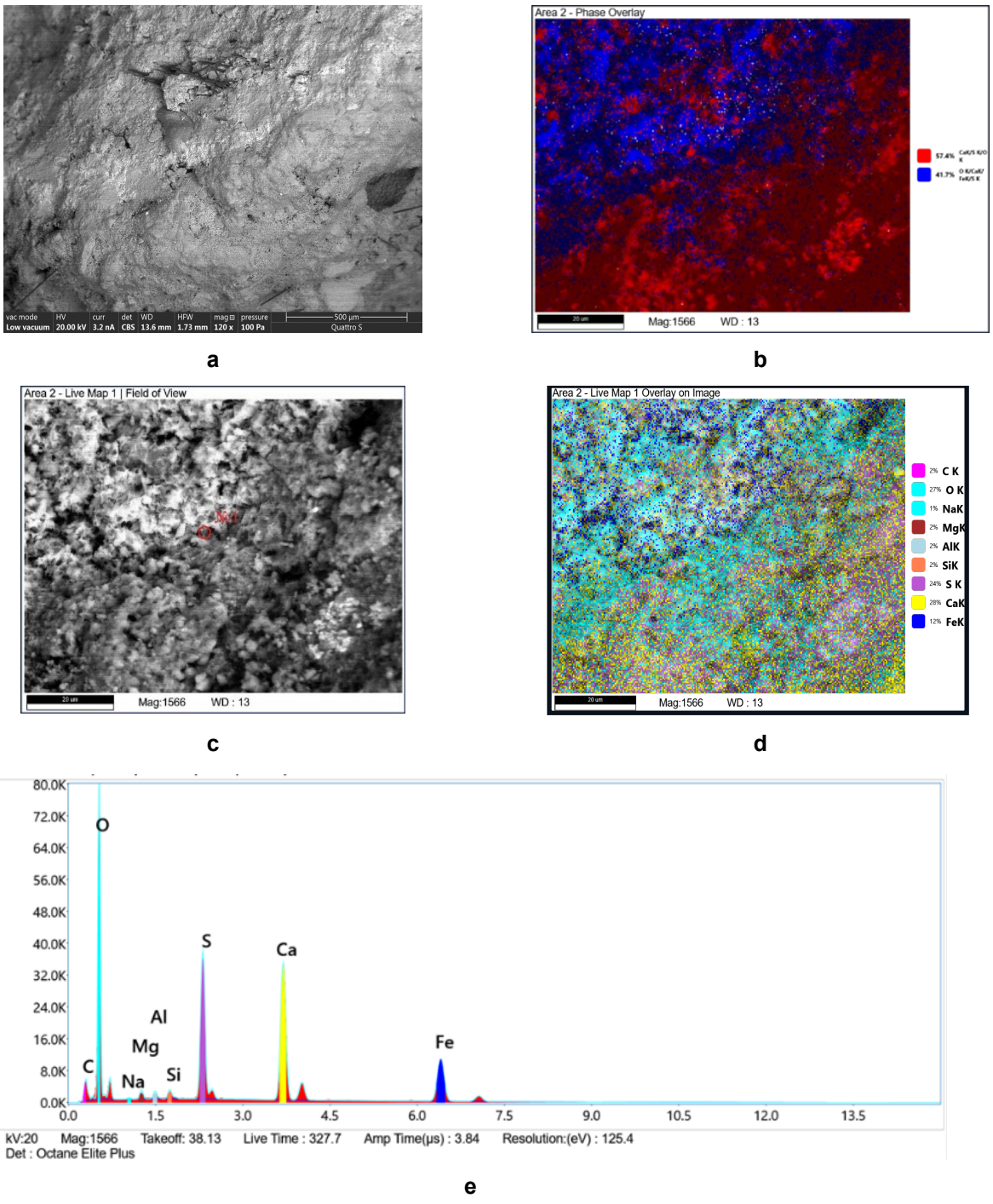

Figure 8. Iron ion migration analysis, sampling Zone No. 2, after several heating cycles: a – general structure view, boundary of Zones No. 2 and No. 3, at 120x magnification; b – chemical compound mapping (red – CaK/S K/OK, blue – OK/ CaK/ FeK/ SK); c – microstructure of elemental mapping area at higher magnification; d – element mapping of area c; e – quantitative analysis at point 1.

The mapping obtained as a result of energy-dispersive analysis (Figs. 8b, 8d, and 8e) confirmed the active migration of iron ions into the structure of the mineral matrix and the presence of Zones No. 1 and No. 2 with a microstructure different from Zone No. 3, formed due to changes in the conditions of structure formation during heating of the product. This process is caused by electrochemical corrosion of the heating element (reinforcement) due to the presence of a significant amount of bound and free water in the hydrated sulfate-containing binder. In this case, heating determines the emergence of conditions for the accelerated formation of iron-containing compounds, including iron oxides and hydroxides (Figs. 8b, 8d, and 8e).

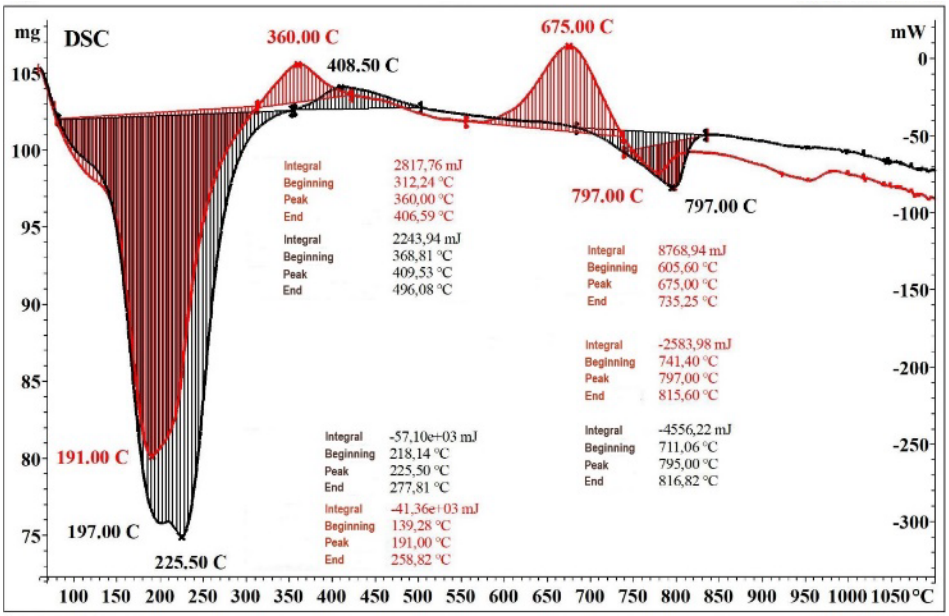

Figure 9.DSC analysis of samples on the 28th day of hardening, after several heating/cooling cycles: red – modified composition; black – control composition.

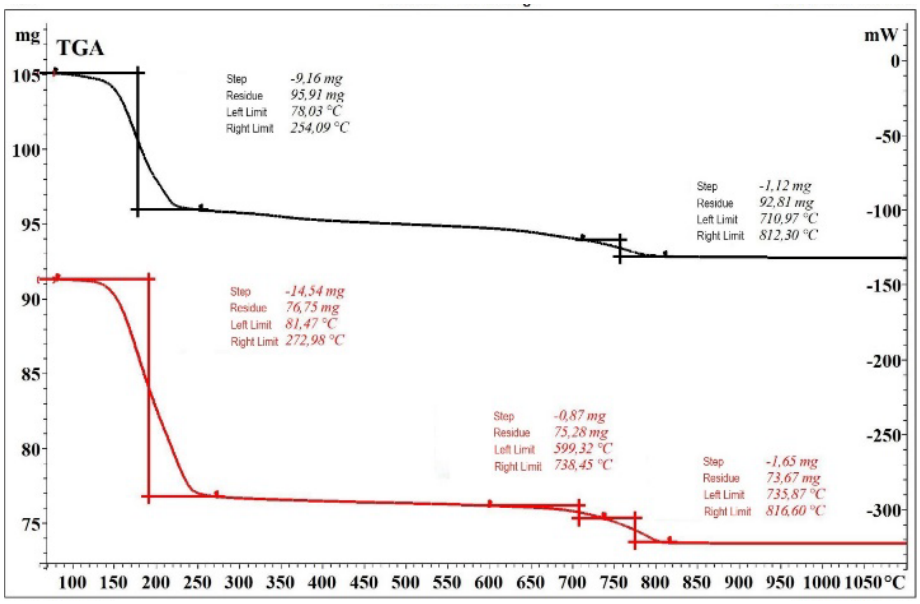

Figure 10. TG analysis of samples on the 28th day of hardening, after several heating/cooling cycles: red – modified composition; black – control composition.

To confirm the insignificant effect of heating the product on the modified matrix located at a distance from the heating elements, DTA/TG analysis was performed on a sample taken from Zone No. 3 after several heating/cooling cycles.

Comparative analysis of differential scanning calorimetry, thermogravimetric analysis of the control and modified samples showed that in the temperature range up to 280 °C, dehydration of crystal hydrate water occurs, characterized by a significant mass loss of 15.9 % for the modified composition and 8.7 % for the control one. In addition, a strong exothermic effect with a maximum at a temperature of 675 °C is observed on the DSC curve for the modified composition. In the studied temperature range, phase transformations of carbon with the release of heat are absent [35], the obtained data probably demonstrate the result of the process of interaction of carbon with oxygen with the formation of carbon monoxide (oxidation and burnout of the additive).

At 408.5 °C in the control composition and 360 °C in the modified composition, calcium sulfate recrystallizes.

The control and modified compositions exhibit an endothermic effect at 797 °C in the control composition and at 777.3 °C in the modified composition, associated with the dissociation of calcium carbonate.

Thus, the analysis of the obtained data allows us to conclude that carbon fiber can be used as micro-heating elements; the additive provides satisfactory physical and mechanical characteristics, thermophysical parameters, while the modification and subsequent heating of the product are not accompanied by physical and chemical changes.

4. Conclusions

Based on the conducted comprehensive analysis of the influence of heating on the microstructure and properties of the mineral matrix based on a binder of anthropogenic origin, the following was found:

1. The introduction of carbon fiber in the amount of 0.75 % of the binder mass, in combination with a hardening activator, provides mechanical strength of 24.2 MPa and specific volume resistance of 8.5 kOhm·cm. The achieved parameters meet the operational requirements for heated products.
2. The optimal electric current values were determined to be U = 120 V, I = 3 A, providing a uniform temperature gradient over the surface of the product and heating the product by 9.2 °C within 40 minutes. The average power consumption was 660 W/m^2.
3. After several heating/cooling cycles, a lack of adhesion was found between the hydrated fluoroanhydrite matrix and the unprotected steel rod (reinforcement) due to accelerated electrochemical corrosion of the heating element.
4. The degree of negative influence of heating on the structure and composition of the modified mineral matrix was determined depending on the distance to the reinforcing element.
5. Migration of iron ions has been established, determining the degree of destruction of the mineral matrix, which can be tracked by the depth of penetration of iron ions and the influence of electrochemical corrosion products.

Thus, based on the proposed compositions, an economically efficient, low-material-intensive system can be developed for heating residential and industrial premises. However, it is necessary to establish the maximum possible number of heating/cooling cycles of products, to offer effective solutions to reduce the degree of influence of electrochemical corrosion on heating elements.

References

1. Litvinova, T.E., Suchkov, D.V. Comprehensive Approach to the Utilisation of Technogenic Waste from the Mineral Resource Complex. Mining Informational and Analytical Bulletin. 2022. 6–1. Pp. 331–48. DOI: 10.25018/0236_1493_2022_61_0_331
2. Alfimova, N., Pirieva, S., Titenko, A. 2021. Utilization of gypsum-bearing wastes in materials of the construction industry and other areas. Construction Materials and Products. 4 (1). Pp. 5–17. DOI: 10.34031/2618-7183-2021-4-1-5-17
3. Alfimova, N.I., Pirieva, S.Yu., Levitskaya, K.M., Kozhukhova, N.I. Optimization of Parameters for the Production of Gypsum Binders Based on Gypsum-Containing Waste. Lecture Notes in Civil Engineering. 2023. 307. Innovations and Technologies in Construction. BUILDINTECH BIT 2022. Pp. 148–154. DOI: 10.1007/978-3-031-20459-3_19
4. Petropavlovskaya, V., Sulman, M.G., Novichenkova, T., Kosivtsov, Y.Y., Zavadko, M., Petropavlovskii, K. Gypsum Composition with a Complex Based on Industrial Waste. Chemical Engineering Transactions. 2021. 88. Pp. 1009–1014. DOI: 10.3303/CET2188168
5. Levickaya, K., Alfimova, N., Nikulin, I., Kozhukhova, N., Buryanov, A. The Use of Phosphogypsum as a Source of Raw Materials for Gypsum-Based Materials. Resources. 2024. 13(5). Article no. 69. DOI: 10.3390/resources13050069
6. Gordina, A.F., Gumenyuk, A.N., Polyanskikh, I.S., Zaripova, R.I. Carbon-Containing Modifier for Fluoranhydrite Binder. Nanotechnologies in Construction. 2022. 14(5). Pp. 381–391. DOI: 10.15828/2075-8545-2022-14-5-381-391
7. Ponomarenko, A.A. Technogenic anhydrite binder for high-strength concrete. Magazine of Civil Engineering. 2021. 107(7). Article no. 10701. DOI: 10.34910/MCE.107.1
8. Alfimova, N.I., Pirieva, S.Yu., Elistratkin, M.Yu., Kozhuhova, N.I., Titenko, A.A. Production methods of binders containing gypsum-bearing wastes: a review. Bulletin of BSTU named after V.G. Shukhov. 2020. 5(11). Pp. 8–23. DOI: 10.34031/2071-7318-2020-5-11-8-23
9. Fedorchuk, Y.M., Tsygankova, T.S. Design methods to reduce the impact of hydrofluoric acid production on the environment. International Journal of Experimental Education. 2014. 1–1. P. 111.
10. Budnikov, P.P., Zorin, S.P. Anhydritovyj Tsement [Anhydrite cement]. Moscow: Promstroyizdat, 1954. 92 p.
11. Yao, G., Cui, T., Jia, Z., Sun, S., Anning, C., Qiu, J., Lyu, X. Effect of Anhydrite on Hydration Properties of Mechanically Activated Muscovite in the Presence of Calcium Oxide. Applied Clay Science. 2020. 196. Article no. 105742. DOI: 10.1016/j.clay.2020.105742
12. Podgorny, D.S., Elistratkin, M.Y., Bondarenko, D.O., Strokova, V.V. Increasing the Radioshielding Properties of Construction Materials in the Microwave Range. Nanotechnologies in Construction. 2024. 16(2). Pp. 100–108. DOI: 10.15828/2075-8545-2024-16-2-100-108
13. Abdullah, A., Mazelan, N., Tadza, M.Y.M., Rahman R.A. The Use of Gypsum and Waste Gypsum for Electrical Grounding Backfill. Lecture Notes in Electrical Engineering. 2021. 666. Pp. 1213–1226. DOI: 10.1007/978-981-15-5281-6_86
14. Zhang, S., Ukrainczyk, N., Zaoui, A., Koenders, E. Electrical Conductivity of Geopolymer-Graphite Composites: Percolation, Mesostructure and Analytical Modeling. Construction and Building Materials. 2024. 411. Article no. 134536. DOI: 10.1016/j.conbuildmat.2023.134536

15. López, F.A., Gázquez, M., Alguacil, F.J., Bolívar, J.P., García-Díaz, I., López-Coto, I. Microencapsulation of Phosphogypsum into a Sulfur Polymer Matrix: Physico-Chemical and Radiological Characterization. Journal of Hazardous Materials. 2011. 192(1). Pp. 234–245. DOI: 10.1016/j.jhazmat.2011.05.010
16. Makul, N. Advanced smart concrete – A review of current progress, benefits and challenges. Journal of Cleaner Production. 2020. 274. Article no. 122899. DOI: 10.1016/j.jclepro.2020.122899
17. Mobili, A., Giosuè, C., Bellezze, T., Revel, G.M., Tittarelli, F. Gasification Char and Used Foundry Sand as Alternative Fillers to Graphene Nanoplatelets for Electrically Conductive Mortars with and without Virgin/Recycled Carbon Fibres. Applied Sciences. 2021. 11(1). Article no. 50. DOI: 10.3390/app11010050
18. Jun, H.-M., Seo, D.-J., Lim, D.-Y., Park, J.-G., Heo, G.-H. Effect of Carbon and Steel Fibers on the Strength Properties and Electrical Conductivity of Fiber-Reinforced Cement Mortar. Applied Sciences. 2023. 13(6). Article no. 3522. DOI: 10.3390/app13063522
19. García-Macíasa, E., Castro-Triguero, R., Ubertini, F. 3D mixed micromechanics-FEM modeling of piezoresistive carbon nanotube smart concrete. Computer Methods in Applied Mechanics and Engineering. 2018. 340. Pp. 396–423. DOI: 10.1016/j.cma.2018.05.037
20. Gordon, A.M., Barrio, M.I.P., Escamilla, A.C. Unveiling the performance of graphene nanofiber additives in gypsum plasters: A solid vs liquid perspective. Journal of Building Engineering. 2024. 87. Article no. 109061. DOI: 10.1016/j.jobe.2024.109061
21. García-Macías, E., D'Alessandro, A., Castro-Triguero, R., Pérez-Mira, D., Ubertini, F. Micromechanics modeling of the electrical conductivity of carbon nanotube cement-matrix composites. Composites Part B: Engineering. 2017. 108. Pp. 451–469. DOI: 10.1016/j.compositesb.2016.10.025
22. Fedorov, V.P. Study of corrosion of reinforcement in gypsum concrete based on high-strength gypsum and methods of its protection: Abstract of thesis for the degree of candidate of technical sciences. Kharkov Engineer-Builder Institute. Kharkov, 1968. 484 p.
23. Kornilova, T.M., Gushcha, E.V., Orehvo, N.K. Corrosion of steel in gypsum concrete. FKS XX: collection of scientific articles. Grodno: Grodno State University, 2012.
24. Tian, Z., Ye, H. Mechanisms underlying the relationship between electrical resistivity and corrosion rate of steel in mortars. Cement and Concrete Research. 2022. 159. Article no. 106867. DOI: 10.1016/j.cemconres.2022.106867
25. Bolzoni, F., Brenna, A., Ormellese, M. Recent advances in the use of inhibitors to prevent chloride-induced corrosion in reinforced concrete. Cement and Concrete Research. 2022. 154. Article no. 106719. DOI: 10.1016/j.cemconres.2022.106719
26. Aguirre-Guerrero, A.M., Robayo-Salazar, R.A., Mejía de Gutiérrez, R. Corrosion resistance of alkali-activated binary reinforced concrete based on natural volcanic pozzolan exposed to chlorides. Journal of Building Engineering. 2021. 33. Article no. 101593. DOI: 10.1016/j.jobe.2020.101593
27. Pan, T., Nguyen, T.A. Shi, X. Assessment of Electrical Injection of Corrosion Inhibitor for Corrosion Protection of Reinforced Concrete. Transportation Research Record. 2008. 2044(1). Pp. 51–60. DOI: 10.3141/2044-06
28. Tuutti, K. Corrosion of steel in concrete. Doctoral Thesis (monograph). Division of Building Material. Swedish Cement and Concrete Research Institute. Stockholm, 1982. 473. p.
29. Dehghanpour, H., Yilmaz, K., Ipek, M. Evaluation of recycled nano carbon black and waste erosion wires in electrically conductive concretes. Construction and Building Materials. 2019. 221. Pp. 109–121. DOI: 10.1016/j.conbuildmat.2019.06.025
30. Liu, X., Qu, M., Nguyen, A.P.T., Dilley, N.R., Yazawa, K. Characteristics of new cement-based thermoelectric composites for low-temperature applications. Construction and Building Materials. 2021. 304. Article no. 124635. DOI: 10.1016/j.conbuildmat.2021.124635
31. Lee, H., Park, S., Kim, D., Chung, W., Heating Performance of Cementitious Composites with Carbon-Based Nanomaterials. 2022. 12. Article no. 716. DOI: 10.3390/cryst12050716
32. Lopanov, A.N., Fanina, E.A., Nesterova, N.V. Differential-Scanning Calorimetry of Graphite and Activated Carbon in Argon. Solid Fuel Chemistry. 2021. 55(2). Pp. 105–109. DOI: 10.3103/S0361521921020051
33. Dudin, M.O., Vatin, N.I., Barabanshchikov, Y.G. Modeling a set of concrete strength in the program ELCUT at warming of monolithic structures by wire. Magazine of Civil Engineering. 2015. 54(2). Pp. 33–45. DOI: 10.5862/MCE.54.4
34. Cherkasova, T.G., Cherkasova, E.V., Tikhomirova, A.V., Gilyazidinova, N.V., Gilyazidinova, N.V., Klyuev, R.V., Karlina, A.I., Skiba, V.Y. Study of Matrix and Rare Elements in Ash and Slag Waste of a Thermal Power Plant Concerning the Possibility of their Extraction. Metallurgist. 2022. 65(11–12). Pp. 1324–1330. DOI: 10.1007/s11015-022-01278-2
35. Rassokhin, A., Ponomarev, A., Shambina, S., Karlina, A. Different types of basalt fibers for disperse reinforcing of fine-grained concrete. Magazine of Civil Engineering. 2022. 109(1). Article no. 10913. DOI: 10.34910/MCE.109.13
36. Bosikov, I.I., Klyuev, R.V., Revazov, V.Ch., Martyushev, N.V. Analysis and evaluation of prospects for high-quality quartz resources in the North Caucasus. Mining Science and Technology (Russia). 2023. 8(4). Pp. 278–289. DOI: 10.17073/2500-0632-2023-10-165
37. Kondratiev, V.V., Karlina, A.I., Guseva, E.A., Konstantinova, M.V., Gorovoy, V.O. Structure of Enriched Ultradisperse Wastes of Silicon Production and Concretes Modified by them. IOP Conference Series: Materials Science and Engineering. 2018. 463(4). Article no. 042064. DOI: 10.1088/1757-899X/463/4/042064
38. Usmanov, R., Mrdak, I., Vatin, N., Murgul, V. Reinforced Soil Beds on Weak Soils. Applied Mechanics and Materials. 2014. 633–634. Pp. 932–935. DOI: 10.4028/www.scientific.net/AMM.633-634.932
39. Wang, X., Wu, Y., Zhu, P., Ning, T. Snow Melting Performance of Graphene Composite Conductive Concrete in Severe Cold Environment. Materials. 2021. 14. Article no. 6715. DOI: 10.3390/ma14216715
40. Farcas, C., Galao, O., Navarro, R., Zornoza, E., Baeza, F.J., Del Moral, B., Pla, R., Garcés, P. Heating and de-icing function in conductive concrete and cement paste with the hybrid addition of carbon nanotubes and graphite products. Smart Materials and Structures. 2021. DOI: 30. Article no. 045010. 10.1088/1361-665X/abe032
41. Kondrat'ev, V.V., Ershov, V.A., Shakhrai, S.G., Ivanov, N.A., Karlina, A.I. Formation and Utilization of Nanostructures Based on Carbon During Primary Aluminum Production. Metallurgist. 2016. 60(7–8). Pp. 877–882. DOI: 10.1007/s11015-016-0380-x
42. Yelemessov, K., Sabirova, L.B., Martyushev, N.V., Malozyomov, B.V., Bakhmagambetova, G.B., Atanova, O.V. Modeling and Model Verification of the Stress-Strain State of Reinforced Polymer Concrete. Materials. 2023. 16(9). Article no. 3494. DOI: 10.3390/ma16093494

43. Amran, M., Onaizi, A.M., Fediuk, R., Vatin N.I., Rashid, R.S.M., Abdelgader, H., Ozbakkaloglu, T. Self-Healing Concrete as a Prospective Construction Material: A Review. Materials. 2022. 15(9). Article no. 3214. DOI: 10.3390/ma15093214

Information about the authors:

***Aleksandr Gumeniuk**, PhD in Technical Sciences*
ORCID: https://orcid.org/0000-0002-2880-8103
E-mail: aleksandrgumenyuk2017@yandex.ru

***Anastasiia Gordina**, PhD in Technical Sciences*
ORCID: https://orcid.org/0000-0001-8118-8866
E-mail: gism56@mail.ru

***Semyon Petrynin**,*
ORCID: https://orcid.org/0009-0009-8950-2907
E-mail: petryninofficial@yandex.ru

***Aleksandr Buryanov**, Doctor of Technical Sciences*
ORCID: https://orcid.org/0000-0002-3331-9443
E-mail: rga-service@mail.ru

***Vadim Skeeba**, PhD in Technical Sciences*
ORCID: https://orcid.org/0000-0002-8242-2295
E-mail: skeeba_vadim@mail.ru

Received 11.07.2024. Approved after reviewing 25.12.2024. Accepted 13.01.2025.